*Inorg. Chem.* **2003**, *42*, 2704–2713


# Model Complexes for Metallated Polythiophenes: Gold(I) and Palladium(II) Complexes of Bis(diphenylphosphino)oligothiophenes

**Olivier Clot,[†] Yumi Akahori,[‡,§] Carolyn Moorlag,[†] Daniel B. Leznoff,*[,§] Michael O. Wolf,*[,†] Raymond J. Batchelor,[§] Brian O. Patrick,[†] and Mikita Ishii[‡]**

*Department of Chemistry, The University of British Columbia, Vancouver, British Columbia, Canada V6T 1Z1, Department of Chemistry, Simon Fraser University, 8888 University Drive, Burnaby, British Columbia, Canada V5A 1S6, and Department of Industrial Chemistry, Meiji University, Higashi-mita, 1-1-1, Tama-ku, Kawasaki-shi, Kanagawa-ken, 214-8571 Japan*

Received June 28, 2002

The preparations of two new phosphinothiophene ligands, 3,3′-bis(diphenylphosphino)-2,2′-bithiophene (dppbt; **1**) and 3,3‴-dihexyl-3′,3″-bis(diphenylphosphino)-2,5′:2′,2″:5″,2‴-quaterthiophene (hdppqt; **2**) are reported. Oxidation of **1** gives 3,3′-bis(diphenylphosphine oxide)-2,2′-bithiophene (**3**), and the crystal structure of this compound was determined. Pd(II) and Au(I) complexes of these ligands have been synthesized and characterized. Crystal structures of [(dppbt)$PdCl_2$] (**1-Pd**), [(hdppqt)$PdCl_2$] (**2-Pd**), [(dppbt)$(AuCl)_2$] (**1-Au**), and [(hdppqt)$(AuCl)_2$] (**2-Au**) were obtained. [(dppbt)$(AuCl)_2$] crystallized in two solid-state forms; crystals grown from $CH_2Cl_2/Et_2O$ show a gold–gold interaction of 3.3221(4) Å, but from $CH_2Cl_2$/toluene, the molecule crystallizes as a toluene adduct (**1-Au-tol**) and does not show any gold–gold interaction. All the complexes were characterized via UV–vis spectroscopy and cyclic voltammetry, and the effect of the metal on the energy of the $\pi$–$\pi^*$ transition and oxidation potential was determined. These data are correlated to the interannular torsion angles in the oligothienyl groups from the crystal structure studies.

## Introduction

Conjugated polymers and oligomers are an important class of materials which are of use in a wide range of applications, including polymer light-emitting diodes,[1] chemical sensors,[2] and thin-film transistors.[3] Many studies have focused on altering the optical and electronic properties of these materials via synthetic modification of the conjugated backbone or substituents. This may be achieved either via steric or electronic influences of the substituent. One approach that has been exploited is the attachment of metal groups to a conjugated backbone so that the metal centers are electronically coupled to the backbone.[4−7] This allows tuning of the electronic properties of the metal and/or backbone, which may have applications in electrocatalysis or chemical sensing involving the pendant metal groups.[7,8]

It has been shown that phosphines are useful in coordinating transition-metal centers to conjugated oligothiophene or polythiophene backbones.[7,9,10] Incorporating pendant bidentate bisphosphines where the two arms of the ligand are on adjacent thiophene rings results in the formation of a seven-membered ring in which the adjacent thiophene rings are immobilized with respect to each other (Scheme 1). The conjugation along the backbone is primarily determined by

* To whom correspondence should be addressed. E-mail: mwolf@chem.ubc.ca (M.O.W.); dleznoff@sfu.ca (D.B.L.). Fax: 604-822-2847 (M.O.W.); 604-291-3765 (D.B.L.).
[†] University of British Columbia.
[‡] Meiji University.
[§] Simon Fraser University.

(1) Kraft, A.; Grimsdale, A. C.; Holmes, A. B. *Angew. Chem., Int. Ed.* **1998**, *37*, 403−428.
(2) McQuade, D. T.; Pullen, A. E.; Swager, T. M. *Chem. Rev.* **2000**, *100*, 2537−2574.
(3) Horowitz, G. *Adv. Mater.* **1998**, *10*, 365−377.
(4) Ley, K. D.; Whittle, C. E.; Bartberger, M. D.; Schanze, K. S. *J. Am. Chem. Soc.* **1997**, 3423−3424.
(5) Wang, Q.; Wang, L.; Yu, L. *J. Am. Chem. Soc.* **1998**, *120*, 12860−12868.
(6) Wolf, M. O. *Adv. Mater.* **2001**, *13*, 545−553.
(7) Weinberger, D. A.; Higgins, T. B.; Mirkin, C. A.; Stern, C. L.; Liable-Sands, L. M.; Rheingold, A. L. *J. Am. Chem. Soc.* **2001**, *123*, 2503−2516.
(8) Kingsborough, R. P.; Swager, T. M. *Prog. Inorg. Chem.* **1999**, *48*, 123−231.
(9) Clot, O.; Wolf, M. O.; Patrick, B. O. *J. Am. Chem. Soc.* **2000**, *122*, 10456−10457.
(10) Clot, O.; Wolf, M. O.; Yap, G. P. A.; Patrick, B. O. *J. Chem. Soc., Dalton Trans.* **2000**, 2729−2737.



10.1021/ic0258328 CCC: $25.00 
Published on Web 03/27/2003

**Scheme 1**

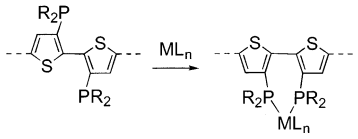

the overlap between the ring $\pi$-systems,[11] and control of polymer properties such as absorption, emission, and conductivity that are dictated by the conjugation are then expected to be directed, in part, by the metal. A related approach has been used to prepare conjugated polymers for use in colorimetric sensors in which binding to a pendant crown ether results in a change in the backbone conformation and thus the color of the material.[12] It is then of interest to construct model complexes in order to probe these effects and to elucidate whether polymers incorporating these groups may possess interesting electronic properties.

Toward this goal, we describe here two new bis(phosphino)thiophene ligands **1** and **2**. We have prepared and determined the structures of Pd(II) and Au(I) complexes containing these ligands, and the characterization of these compounds using UV−vis spectroscopy and cyclic voltammetry is described.

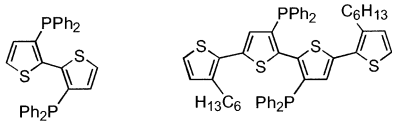

**1** dppbt



**2** hdppqt

## Experimental Section

**General.** All reactions were performed using standard Schlenk techniques with dry solvents under nitrogen. [AuCl(tht)] (tht = tetrahydrothiophene),[13] 2-bromo-3-hexylthiophene,[14] 3,5,3′,5′-tetrabromo-2,2′-bithiophene,[15] and 3,3′-dibromo-2,2′-bithiophene[15] were prepared according to literature procedures. $^1$H and $^{31}$P{$^1$H} NMR experiments were performed on either a Bruker AC-200E or a Bruker AV-300 spectrometer, and spectra were referenced to residual solvent ($^1$H) or external 85% $H_3PO_4$ ($^{31}$P). Electronic absorption spectra were obtained in $CH_2Cl_2$. Microanalyses (C, H, N) were performed either at Simon Fraser University by Mr. Miki Yang or at UBC by Mr. Peter Borda. Electrochemical measurements were conducted on a Pine AFCBP1 bipotentiostat using a Pt disk working electrode, a Pt coil wire counter electrode, and a silver wire reference electrode. An internal reference, either decamethylferrocene (−0.12 V vs SCE) or ferrocene (0.41 V vs SCE),[16] was added to correct the measured potentials with respect to saturated calomel electrode (SCE). The supporting electrolyte was 0.1 M [(*n*-Bu)$_4$N]$PF_6$, which was purified by triple recrystallization from ethanol and dried at 90 °C under vacuum for 3 days. Methylene chloride used in cyclic voltammetry was dried either by refluxing over $CaH_2$ or by passing through an activated alumina tower. $CH_3CN$ was dried over 4 Å molecular sieves.

**3,3′-Bis(diphenylphosphino)-2,2′-bithiophene (dppbt; 1).** To a solution of BuLi (1.6 M, 4.30 mL, 6.80 mmol) in 4 mL of dry THF at −78 °C was slowly added a solution of 3,3′-dibromo-2,2′-bithiophene (1.00 g, 3.10 mmol) in dry THF (4 mL) under nitrogen. The mixture was stirred at −78 °C for 1 h. The temperature was then raised to −50 °C and $PPh_2Cl$ (3.00 g, 13.6 mmol) added dropwise. The cold bath was removed and the reaction mixture allowed to warm to 25 °C and stirred for 1 h. The reaction was then quenched with water and diethyl ether (40 mL) added. The organic phase was washed with water and dried over anhydrous $MgSO_4$ and the solvent removed to leave a yellow solid. The crude product was purified by chromatography on silica gel using a $CH_2Cl_2$/hexanes mixture (6/4 v/v) as eluant. The first band was collected and the solvent removed to yield **1** as an off-white solid. Yield: 0.70 g (46%). $^1$H NMR (200 MHz, $CDCl_3$): $\delta$ 7.36−7.18 (m, 11H), 6.68 (d, $J_{HH}$ = 5.1 Hz, 1H). $^{31}$P{$^1$H} NMR (81.015 MHz, $CDCl_3$): $\delta$ −26.4 (s). Anal. $C_{32}H_{24}P_2S_2$ requires: C, 71.91; H, 4.49. Found: C, 71.69; H, 4.65%.

**3,3′-Bis(diphenylphosphine oxide)-2,2′-bithiophene (3).** To a solution of **1** (1.0 g) in $CHCl_3$ (50 mL) and acetone (50 mL) was added 30% $H_2O_2$ (0.4 mL). A white solid began to precipitate immediately, and the mixture stirred for 1 h. The solid was collected by filtration, redissolved in $CHCl_3$, filtered, and precipitated with acetone to give a white solid. Yield: 0.54 g (51%). $^1$H NMR (200 MHz, $CDCl_3$): $\delta$ 7.71 (ddd, $J$ = 1.6, 8.2, 14.0 Hz, 8H), 7.53−7.36 (m, 12H), 7.18 (dd, $J_{HH}$ = 5.4 Hz, $J_{HP}$ = 2.2 Hz, 2H), 6.65 (dd, $J_{HH}$ = 5.4 Hz, $J_{HP}$ = 4.4 Hz, 2H). $^{31}$P{$^1$H} NMR (81.015 MHz, $CDCl_3$): $\delta$ 20.5 (s). Anal. $C_{32}H_{24}O_2P_2S_2$ requires: C, 67.83; H, 4.27. Found: C, 67.59; H, 4.32%.

**3,3‴-Dihexyl-3′,3″-dibromo-2,5′:2′2″:5″,2‴-quaterthiophene (4).** A solution of 2-bromo-3-hexylthiophene (7.34 g, 30 mmol) in THF was added dropwise to a mixture of magnesium (1.41 g, 58 mmol) and trace iodine in THF (30 mL) at reflux, and then heated further to reflux for 2 h. The resulting solution was added dropwise at 25 °C via cannula to a mixture of 3,5,3′,5′-tetrabromo-2,2′-bithiophene (5.72 g, 12 mmol) and [Pd(dppf)$Cl_2$] (200 mg, 0.6%) in diethyl ether (30 mL) and toluene (20 mL), and heated to reflux for 3 h. The reaction was then quenched with saturated aqueous ammonium chloride (50 mL), and filtered through Celite to remove insoluble material. $CH_2Cl_2$ (50 mL) was then added and the organic phase separated. The aqueous phase was extracted with $CH_2Cl_2$. The combined organic phases were washed with saturated $NaHCO_3$ solution and $H_2O$ and dried with anhydrous $MgSO_4$ and the solvent removed to give a thick orange oil. The crude product was purified by column chromatography on silica gel with hexanes as eluant. The first three bands contained small amounts of unreacted 3,5,3′,5′-tetrabromo-2,2′-bithiophene, 3-hexylthiophene, and monosubstituted terthiophene side product, respectively. The fourth band contained the desired product **4**, and removal of solvent left a bright-yellow, waxy solid. Penta- and hexathiophene products were also isolated in subsequent bands. Yield: 4.02 g (52%). $^1$H NMR (200 MHz, $CDCl_3$): $\delta$ 7.23 (d, $J_{HH}$ = 5.2 Hz), 2H), 7.09 (s, 2H), 6.96 (d, $J_{HH}$ = 5.2 Hz, 2H), 2.79 (t, $J_{HH}$ = 7.7 Hz, 4H), 1.64 (m, 4H), 1.34 (m, 12H), 0.90 (t, 6.3 Hz, 6H). Anal. $C_{28}H_{32}Br_2S_4$ requires: C, 51.22; H, 4.91. Found: C, 51.34; H, 4.72%.

**3,3‴-Dihexyl-3′,3″-bis(diphenylphosphino)-2,5′:2′,2″:5″,2‴-quaterthiophene (hdppqt; 2).** To a suspension of **4** (1.0 g, 1.52 mmol) in diethyl ether (30 mL) at −78 °C was added a solution of

(11) Brédas, J. L.; Street, G. B.; Thémans, B.; Andre, J. M. *J. Chem. Phys.* **1985**, *83*, 1323−1329.
(12) Marsella, M. J.; Swager, T. M. *J. Am. Chem. Soc.* **1993**, *115*, 12214−12215.
(13) Usón, R.; Laguna, A. *Organomet. Synth.* **1986**, *3*, 322−342.
(14) Kellogg, R. M.; Schaap, A. P.; Harper, E. T.; Wynbert, H. *J. Org. Chem.* **1968**, *33*, 2902−2909.
(15) Khor, E.; Ng, S. C.; Li, H. C.; Chai, S. *Heterocycles* **1991**, *32*, 1805−1812.
(16) Robbins, J. L.; Edelstein, N.; Spencer, B.; Smart, J. C. *J. Am. Chem. Soc.* **1982**, *104*, 1882−1893.

BuLi (1.6 M, 2.10 mL, 3.35 mmol) in dry THF. The mixture was slowly warmed until the suspended solids dissolved at −30 °C to give an orange solution, and $PPh_2Cl$ (1.34 g, 6.09 mmol) was subsequently added. After 5 min (−30 °C), a yellow precipitate formed, and the mixture was slowly allowed to warm to room temperature and stirred for 1 h. The reaction was quenched with water and dried over anhydrous $MgSO_4$, and the solvent was removed to leave a dark-yellow mixture. The crude product was purified by chromatography on silica gel using hexanes/$CH_2Cl_2$ mixture (4:1) as eluent. The first two bands contained starting materials, and the third band contained the monosubstituted side product. Removal of solvent from the fourth band yielded **2** as a dark-yellow oil. Yield: 0.91 g (61%). $^1$H NMR (200 MHz, $CDCl_3$): $\delta$ 7.31 (m, 10H), 7.10 (d, $J_{HH}$ = 5.1 Hz, 1H), 6.85 (d, $J_{HH}$ = 5.1 Hz, 1H), 6.65 (s, 1H), 2.55 (m, 2H), 1.56−1.07 (m, 8H), 0.88 (m, 3H). $^{31}$P{$^1$H} NMR (81.015 MHz, $CDCl_3$): $\delta$ −25.1 (s). Anal. $C_{52}H_{52}P_2S_4$ requires: C, 72.06; H, 6.00. Found: C, 72.34; H, 6.23%.

**[(Dppbt)PdCl$_2$] (1-Pd).** A warm solution of $PdCl_2$ (50.0 mg, 0.28 mmol) in water (3 mL) and concentrated HCl (0.05 mL) was slowly added to **1** (320 mg, 0.60 mmol) in an ethanol/acetonitrile mixture (10/3 mL) at 50 °C. The mixture turned yellow immediately and was stirred for 1 h at 50 °C after which time the mixture was filtered warm to remove any unreacted ligand. The yellow filtrate was concentrated to ∼3−4 mL, causing a yellow solid to precipitate out which was collected by filtration. The crude material was further purified by chromatography on a short column of neutral alumina eluting first with $CH_2Cl_2$, and then with acetone to elute **1-Pd** in a yellow band. One recrystallization from $CH_2Cl_2$/hexanes yielded **1-Pd** as yellow microcrystals. Yield: 151 mg (76%). $^1$H NMR (200 MHz, $CDCl_3$): $\delta$ 7.96−7.64 (m, 4H), 7.56−7.31 (m, 6H), 7.00 (dd, $J_{HH}$ = 5.4 Hz, $J_{HP}$ = 1.7 Hz, 1H), 6.29 (dd, $J_{HH}$ = 5.4 Hz, $J_{HP}$ = 2.9 Hz, 1H). $^{31}$P{$^1$H} NMR (81.015 MHz, $CDCl_3$): $\delta$ 17.9 (s). Anal. $C_{32}H_{24}Cl_2P_2PdS_2$ requires: C, 53.98; H, 3.37. Found: C, 53.61; H, 2.99%.

**[(Hdppqt)PdCl$_2$] (2-Pd).** A warm solution of $PdCl_2$ (17.9 mg, 0.10 mmol) in water (2 mL) and concentrated HCl (0.02 mL) was slowly added to **2** (96.0 mg, 0.11 mmol) in an ethanol/acetonitrile mixture (8/3 mL) at 50 °C. The mixture turned dark orange immediately and was stirred for 1 h after which time water was added to precipitate a yellow solid. The slurry was stirred for 1 h at 50 °C and filtered warm to collect an orange solid that was washed with water and hexanes. Recrystallization from $CH_2Cl_2$/hexanes yielded **2-Pd** as a light orange powder. Yield: 51 mg (48%). $^1$H NMR (200 MHz, $CDCl_3$): $\delta$ 8.05−7.62 (m, 4H), 7.58−7.27 (m, 6H), 7.14 (d, $J_{HH}$ = 5.1 Hz, 1H), 6.84 (d, $J_{HH}$ = 5.1 Hz, 1H), 6.23 (d, $J_{HP}$ = 2.8 Hz, 1H), 2.45−2.21 (m, 2H), 1.51−1.10 (m, 8H), 1.03−0.76 (m, 3H). $^{31}$P{$^1$H} NMR (81.015 MHz, $CDCl_3$): $\delta$ 17.5 (s). Anal. $C_{52}H_{52}Cl_2P_2PdS_4$ requires: C, 59.80; H, 4.98. Found: C, 59.67; H, 5.12%.

**[(Dppbt)(AuCl)$_2$] (1-Au).** A $CH_2Cl_2$ solution (10 mL) of **1** (0.10 g, 0.19 mmol) was added dropwise to a $CH_2Cl_2$ solution (20 mL) of [AuCl(tht)] (0.12 g, 0.38 mmol). The yellow solution rapidly decolorized and was stirred for 30 min, and then, the solvent was removed in vacuo. Recrystallization of the resulting solid from 1:1 $CH_2Cl_2$/ether gave air-stable colorless needles of **1-Au** suitable for X-ray structural analysis. Yield: 90 mg (49%). $^1$H NMR (200 MHz, $CDCl_3$): $\delta$ 7.65−7.45 (m, 4H), 7.45−7.25 (m, 7H), 6.68 (d, $J_{HH}$ = 5.1 Hz, 1H). $^{31}$P{$^1$H} NMR (81.015 MHz, $CDCl_3$): $\delta$ 13.8 (s). Anal. $C_{32}H_{24}Au_2Cl_2P_2S_2$ requires: C, 38.46; H, 2.42. Found: C, 38.81; H, 2.79. Recrystallization from $CH_2Cl_2$/toluene gave air-stable, colorless blocks of (dppbt)$(AuCl)_2\cdot C_7H_8$ (**1-Au-tol**), which was also structurally characterized. Partial desolvation of **1-Au-tol** hindered the acquisition of reproducible elemental analysis data.

**[(Hdppqt)(AuCl)$_2$] (2-Au).** A $CH_2Cl_2$ solution (10 mL) of **2** (0.05 g, 0.06 mmol) was added dropwise to a solution of [AuCl(tht)] (0.038 g, 0.12 mmol) in $CH_2Cl_2$ (20 mL). The yellow/orange solution was stirred for 30 min, and then, the solvent was removed in vacuo. Recrystallization of the resulting solid from 1:1 $CH_2Cl_2$/hexanes at −20 °C gave air-stable red plates of [(hdppqt)$(AuCl)_2$] (**2-Au**) suitable for X-ray structural analysis. Yield: 44 mg (56%). $^1$H NMR (200 MHz, $CDCl_3$): $\delta$ 7.70 (m, 4H), 7.47 (m, 6H), 7.17 (d, $J_{HH}$ = 5.1 Hz, 1H), 6.86 (d, $J_{HH}$ = 5.1 Hz, 1H), 6.66 (d, $J_{HP}$ = 2.8 Hz, 1H), 2.50 (m, 2H), 1.56−1.17 (m, 8H), 0.88 (t, 3H). $^{31}$P{$^1$H} NMR (81.015 MHz, $CDCl_3$): $\delta$ 15.3 (s). Anal. $C_{52}H_{54}Au_2Cl_2P_2S_4$ requires: C, 46.82; H, 4.09. Found: C, 46.69; H, 3.97.

**X-ray Crystallographic Analyses.** Data for the X-ray crystallographic analyses of **1-Pd**, **2-Pd**, **1-Au**, **2-Au**, and **3** were all collected on a Rigaku/ADSC CCD diffractometer; data for **1-Au-tol** were collected on an Enraf Nonius CAD4F diffractometer. For **1-Pd** and **1-Au**, data were collected and processed using the d*TREK program[17] and were subsequently corrected for Lorentz and polarization effects. The structures were solved using direct methods[18] and expanded using Fourier techniques.[19] Molecules of **1-Pd** crystallize in space group $P2_1/n$ with one-half of a molecule of methylene chloride in the asymmetric unit, that is disordered in two orientations about an inversion center. Molecules of **1-Au** crystallize in space group $C2/c$ with two molecules of methylene chloride in the asymmetric unit.

For **1-Au-tol**, the data were corrected empirically for the effects of absorption.[20] Data reduction included corrections for Lorentz and polarization effects. Coordinates and anisotropic displacement parameters were refined for all non-hydrogen atoms. The maximum peak (0.7(2) e/Å$^3$) in the final electron density difference map was located 1.00 Å from Au. The programs used for absorption corrections, data reduction, structure solution, and graphical output were from the *NRCVAX* Crystal Structure System.[21] The structure was refined using *CRYSTALS*.[22] Complex scattering factors for neutral atoms[23] were used in the calculation of structure factors.

For **2-Au**, the structure was solved by direct methods.[18] Both hexyl groups display considerable thermal motion. One group, C(17)−C(22), was modeled in two orientations using isotropic thermal parameters. The second group, C(23)−C(28), was modeled in one orientation using anisotropic thermal parameters. In addition, the material crystallizes with 1.5 molecules of toluene in the asymmetric unit. One solvent molecule was modeled using rigid group restraints with isotropic thermal parameters. All calculations were carried out using teXsan[24] and SHELXL-97.[25] For **2-Pd**, both

(17) *Area Detector Software*, Version 4.13; Molecular Structure Corporation, The Woodlands, Texas, 1996−1998.
(18) Altomare, A.; Burla, M. C.; Camalli, M.; Cascarano, G. L.; Giacovazzo, C.; Guagliardi, A.; Moliterni, A. G. G.; Polidori, G.; Spagna, R. *J. Appl. Crystallogr.* **1999**, *32*, 115−119.
(19) Beurskens, P. T.; Admiraal, G.; Beurskens, G.; Bosman, W. P.; de Gelder, R.; Israel, R.; Smits, J. M. M. *The DIRDIF-94 Program System, Technical Report of the Crystallography Laboratory*; University of Nijmegen, The Netherlands, 1994.
(20) North, A. C. T.; Philips, D. C.; Mathews, F. S. *Acta Crystallogr.* **1968**, *A24*, 351−359.
(21) Gabe, E. J.; LePage, Y.; Charland, J.-P.; Lee, F. L.; White, P. S. *J. Appl. Crystallogr.* **1989**, *22*, 384−387.
(22) Watkin, D. J.; Prout, C. K.; Carruthers, J. R.; Betteridge, P. W.; Cooper, R. I. *CRYSTALS Issue 11*; Chemical Crystallography Laboratory, University of Oxford: Oxford, England, 1999.
(23) *International Tables for X-ray Crystallography*; Kynoch Press: Birmingham, England, 1975; Vol. IV, p 99.
(24) *teXsan: Crystal Structure Analysis Package*; Molecular Structure Corporation, The Woodlands, Texas, 1985 and 1992.

**Table 1.** Crystallographic Data

| | 1-Pd | 2-Pd | 1-Au | 1-Au-tol | 2-Au | 3 |
|---|---|---|---|---|---|---|
| formula | $C_{32.5}H_{25}S_2P_2Cl_3Pd$ | $C_{52}H_{52}P_2S_4Cl_2Pd$ | $C_{34}H_{28}S_2P_2Cl_6Au_2$ | $C_{39}H_{32}Au_2Cl_2P_2S_2$ | $C_{65.2}H_{64}P_2Cl_2Au_2$ | $C_{32.75}H_{25.50}P_2S_2Cl_{1.50}O_2$ |
| mol wt | 754.38 | 1044.48 | 1169.31 | 1091.58 | 1516.29 | 630.31 |
| *T*, K | 173(1) | 173(1) | 198(1) | 293(1) | 173(1) | 298(1) |
| space group | $P2_1/n$ | $P\bar{1}$ | $C2/c$ | $C2/c$ | $P2_1/c$ | $P\bar{1}$ |
| *a*, Å | 11.3597(3) | 13.6973(8) | 13.1073(9) | 15.4256(23) | 11.1645(3) | 9.992(3) |
| *b*, Å | 15.2372(4) | 13.7726(9) | 17.672(1) | 13.8425(14) | 19.043(5) | 10.943(3) |
| *c*, Å | 17.5400(7) | 14.2939(8) | 17.192(1) | 19.425(3) | 29.733(4) | 14.832(7) |
| α, deg | | 73.154(8) | | | | 76.48(1) |
| *β*, deg | 93.21(1) | 76.805(9) | 99.76(1) | 112.314(12) | 91.248(1) | 81.14(2) |
| *γ*, deg | | 73.740(9) | | | | 85.04(2) |
| *V*, Å$^3$ | 3031.2(1) | 2445.6(3) | 3924.6(4) | 3837.1 | 6320(1) | 1555.9(9) |
| $\rho_c$ (g cm$^{-3}$) | 1.653 | 1.418 | 1.979 | 1.890 | 1.593 | 1.345 |
| *Z* | 4 | 2 | 4 | 4 | 4 | 2 |
| $\mu$ (Mo Kα) (mm$^{-1}$) | 1.144 | 7.60 | 8.11 | 7.97 | 4.960 | 4.31 |
| R1,[a] wR2[b] [$I > 3\sigma(I)$] | 0.024, 0.031 | 0.041, 0.082 | 0.028, 0.038 | 0.027, 0.027 | 0.047, 0.090 | 0.101, 0.120 |
| R1,[a] wR2[b] (all data) | 0.042, 0.068 | 0.073, 0.089 | 0.051, 0.080 | | 0.117, 0.109 | 0.206, 0.246 |

[a] $R = \sum||F_o| - |F_c||/\sum|F_o|$. [b] $R_w = \{\sum[w(F_o^2 - F_c^2)^2]/\sum[w(F_o^2)^2]\}^{1/2}$.

hexyl groups are disordered, and each was modeled in two orientations, with the major disordered fragment refined anisotropically and the minor fragments isotropically. Hydrogen atoms were placed in calculated positions.

For **3**, data were collected and processed using the d*TREK program.[17] Complex **3** crystallizes in space group $P\bar{1}$ with one solvent molecule in the asymmetric unit. The structure was solved by direct methods[18] and refined using teXsan.[24] All non-hydrogen atoms were refined anisotropically, while all hydrogen atoms were placed in calculated positions. Subsequent refinements revealed that the solvent molecule was only partially occupied throughout the lattice, with a population of approximately 0.75. The relatively high residuals (R1 = 0.101, wR2 = 0.246) may be due to crystal deterioration, as a result of loss of solvent from the lattice. The crystal data for all six structures are collected in Table 1.

## Results and Discussion

**Ligand Syntheses.** The preparative route used to obtain diphosphines **1** and **2** is shown in Scheme 2. Compound **1** was prepared by addition of the previously prepared 3,3′-dibromo-2,2′-bithiophene to a solution of *n*-butyllithium in THF at −78 °C. This order of addition was necessary due to the poor solubility of the dibromide in THF at low temperatures. The resulting lithium salt was then treated with excess $PPh_2Cl$ at −50 °C. The excess phosphine and higher temperature are necessary to avoid scrambling of the lithium on the oligothienyl group,[26,27] which would be expected to reduce the selectivity of the reaction. Compound **1** was isolated as an off-white powder that is poorly soluble in nonpolar solvents and stable in air. The bis(phosphine oxide)-**3** was readily prepared by oxidation with hydrogen peroxide, and an X-ray crystal structure of this molecule was determined on crystals grown from methylene chloride (Figure 1). Bond lengths and angles are collected in Table 2. The sterically demanding phosphine oxide substituents force the thiophene rings to adopt close to a S-*anti* conformation in the solid state, with an interannular torsion angle (∠S−C−C−S) of 124.1(8)°.

**Scheme 2**

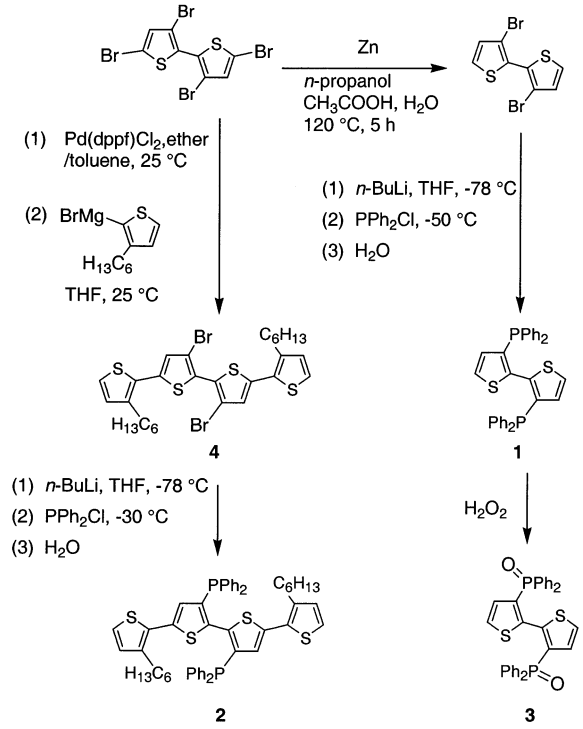


We were also interested in preparing a derivative of **1** with a longer oligothienyl group in order to explore the effect of this on the spectroscopic and electrochemical properties of complexes containing the same metal binding site. Our initial attempts were to prepare an unsubstituted quaterthiophene derivative of **1**; however, these were unsuccessful due to poor solubility. To circumvent these difficulties, we chose to target compound **2** that carries two hexyl substituents to enhance its solubility in organic solvents. Compound **2** was prepared from the quaterthiophene **4** and isolated by column chromatography as a bright yellow solid.

(25) *SHELXL-97*; Sheldrick, G. M., University of Göttingen, Göttingen, Germany, 1997.

(26) Ng, S.-C.; Chan, H. S. O.; Huang, H.-H.; Swee-How, R. *J. Chem. Res. (S)* **1996**, 232−233.

(27) Folli, U.; Goldoni, F.; Iarossi, D.; Mucci, A.; Schenetti, L. *J. Chem. Res. (S)* **1996**, 69.

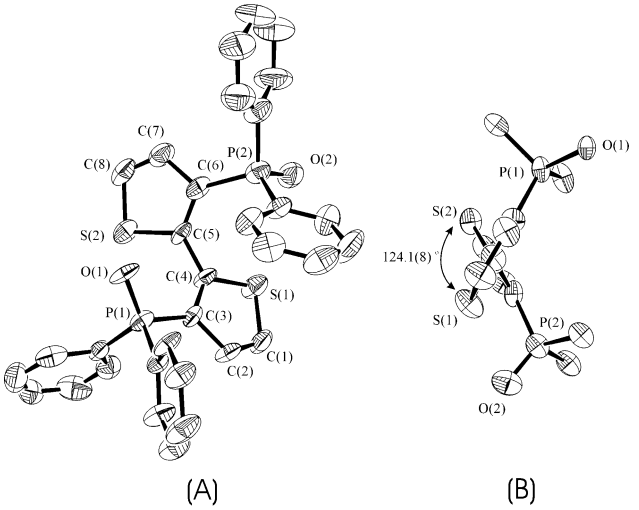


**Figure 1.** (a) ORTEP view of **3**. The hydrogen atoms are omitted for clarity, and thermal ellipsoids are drawn at 50% probability. (b) ORTEP view down C(4)−C(5) axis illustrating the interannular torsion angle (phenyl groups omitted for clarity).

**Table 2.** Selected Bond Lengths and Angles for **3**

| | | | |
|---|---|---|---|
| | Distances, Å | | |
| P(1)−O(1) | 1.495(6) | C(6)−C(7) | 1.48(1) |
| P(2)−O(2) | 1.475(7) | C(4)−C(5) | 1.46(1) |
| P(1)−C(3) | 1.762(9) | S(1)−C(1) | 1.706(9) |
| P(2)−C(6) | 1.80(1) | S(1)−C(4) | 1.704(9) |
| C(5)−C(6) | 1.41(2) | C(1)−C(2) | 1.36(1) |
| S(2)−C(5) | 1.70(1) | C(2)−C(3) | 1.46(1) |
| S(2)−C(8) | 1.73(1) | C(3)−C(4) | 1.41(1) |
| C(7)−C(8) | 1.25(2) | | |
| | Angles, deg | | |
| O(2)−P(2)−C(6) | 117.8(6) | S(1)−C(1)−C(2) | 111.2(6) |
| O(1)−P(1)−C(3) | 114.9(4) | P(1)−C(3)−C(4) | 127.0(6) |
| S(2)−C(5)−C(6) | 111.1(6) | P(1)−C(3)−C(2) | 125.4(7) |
| S(2)−C(8)−C(7) | 112.0(8) | P(2)−C(6)−C(5) | 126.4(6) |
| S(1)−C(4)−C(3) | 113.3(6) | P(2)−C(6)−C(7) | 124.7(8) |

**Scheme 3**

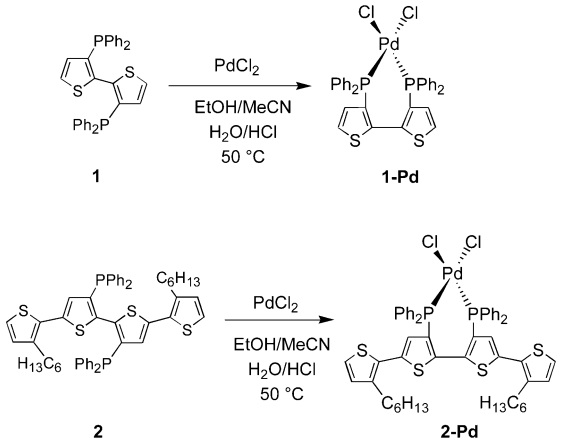


**Palladium Complexes.** In order to explore the coordination of **1** and **2** to transition metals, we reacted these compounds with Pd(II) and Au(I) precursors. Reaction of $PdCl_2$ with a slight excess of **1** or **2** in an ethanol/water mixture at 50 °C yielded **1-Pd** and **2-Pd**, respectively (Scheme 3). For complex **1-Pd**, the ethanol was removed resulting in precipitation of a solid from the solution, which was collected by filtration and washed with water and hexanes. Chromatography on a short neutral alumina column was used to separate excess ligand from **1-Pd**. Recrystallization of the resulting solid from $CH_2Cl_2$/hexanes yielded **1-Pd** as yellow, air-stable microcrystals. Complex **2-Pd** was purified by precipitation from the reaction mixture followed by filtration and washed with water and hexanes. The crude material was further purified by recrystallization from a $CH_2Cl_2$/hexanes mixture. Complex **2-Pd** was obtained as an orange, air-stable powder, which is soluble in polar solvents such as methylene chloride and chloroform.

The $^{31}P\{^1H\}$ NMR spectra of **1-Pd** and **2-Pd** contain singlets at $\delta$ 17.9 and 17.5, respectively. Crystals of **1-Pd** were grown from layered $CH_2Cl_2$/hexanes, and its solid-state structure was determined by X-ray crystallography. The structure of **1-Pd** (Figure 2) shows that the bis(phosphine) ligand chelates to one palladium center via the two phosphines, forming a seven-membered ring with a P−Pd−P bite angle of 93.20(2)°. The Pd(II) center lies in a distorted square planar geometry with the cis chlorine atoms slightly raised above the (P−Pd−P) plane. Selected bond lengths and angles are shown in Table 3. Coordination of **1** to Pd forces the sulfur atoms of the bithienyl group close to a *syn* conformation with an intrannular torsion angle of 51.1(2)°.

The solid-state structure of **2-Pd** is shown in Figure 3, and selected bond lengths and angles are shown in Table 4. There are three distinct interannular torsion angles in **2-Pd**. The central, internal pair of rings are locked at 56.6(3)°, slightly greater than the comparable angle in **1-Pd**. The outer rings are also twisted at similar angles, 58.8(3)° and 69.0(3)°. All four of the rings are oriented approximately S-*syn* to each other, with the sulfur atoms alternating above and below a plane along the quaterthiophene moiety. Most quaterthiophenes are nearly planar in the solid-state, although deviations are sometimes observed due to steric interactions between substituents.[28] The C(8)−C(9) bond in **2-Pd** is shorter (1.452(4) Å) than either of the two other interannular C−C bonds in this structure, but comparable to the interannular bond length in **1-Pd**. It is possible that this shorter bond is indicative of enhanced conjugation between the inner two rings in this oligomer; however, structural effects due to the formation of the metallacycle may also result in some distortion of this bond.

**Gold Complexes.** [(dppbt)$(AuCl)_2$] (**1-Au**) was synthesized via the reaction of **1** with [AuCl(tht)] (Scheme 4). The $^{31}P\{^1H\}$ NMR spectrum of **1-Au** contains one singlet at $\delta$ 13.8, and the elemental analysis is consistent with two Au centers per ligand. Attempts to synthesize the monogold(I) complex [(dppbt)(AuCl)], as was obtained for palladium(II), lead to mixtures, with bimetallic **1-Au** being the major product. Two solid-state structures were established for **1-Au**; in both cases, each gold(I) center binds to one phosphine and one chloride in a nearly linear geometry. The first structure was determined from crystals grown from $CH_2Cl_2/Et_2O$ and shows a gold−gold interaction of 3.3221(4) Å (Figure 4).[29,30] The second one, established from

(28) Lukevics, E.; Barbarella, G.; Arsenyan, P.; Belyakov, S.; Pudova, O. *Chem. Heterocycl. Compd. (N.Y.)* **2000**, *36*, 630−662.
(29) Pathaneni, S. S.; Desiraju, G. R. *J. Chem. Soc., Dalton Trans* **1993**, 319−322.

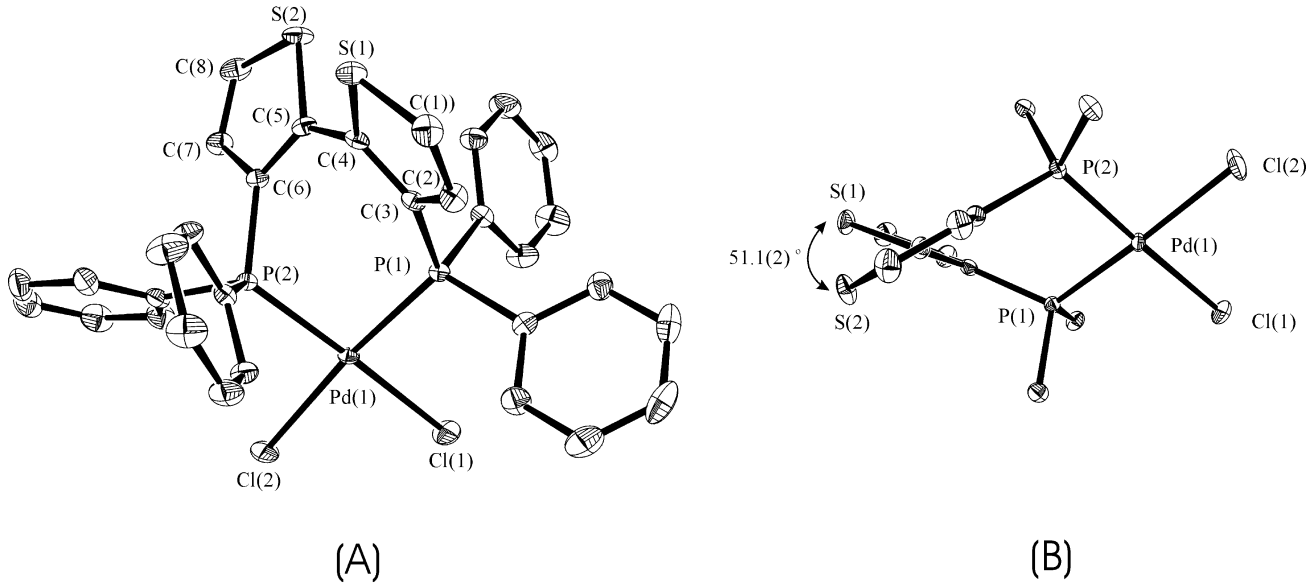


**Figure 2.** (a) ORTEP view of **1-Pd**. The hydrogen atoms are omitted for clarity, and thermal ellipsoids are drawn at 50% probability. (b) ORTEP view down C(4)−C(5) axis illustrating the interannular torsion angle (phenyl groups omitted for clarity).

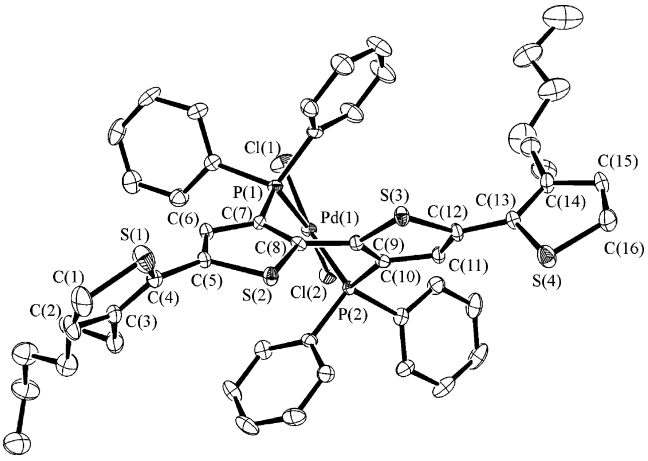


**Figure 3.** ORTEP view of **2-Pd**. The hydrogen atoms are omitted for clarity, and thermal ellipsoids are drawn at 50% probability.

**Table 3.** Selected Bond Lengths and Angles for **1-Pd**

| | | | |
|---|---|---|---|
| | Distances, Å | | |
| Pd(1)−Cl(1) | 2.3536(6) | Pd(1)−Cl(2) | 2.3445(7) |
| Pd(1)−P(1) | 2.2889(6) | Pd(1)−P(2) | 2.2595(6) |
| P(1)−C(3) | 1.832(2) | P(2)−C(6) | 1.823(2) |
| S(1)−C(1) | 1.707(3) | S(1)−C(4) | 1.723(2 |
| C(1)−C(2) | 1.355(3) | C(2)−C(3) | 1.432(3) |
| C(3)−C(4) | 1.379(3) | C(4)−C(5) | 1.456(3) |
| S(2)−C(5) | 1.730(2) | S(2)−C(8) | 1.704(3) |
| C(5)−C(6) | 1.371(3) | C(6)−C(7) | 1.434(3) |
| C(7)−C(8) | 1.353(4) | | |
| | Angles, deg | | |
| Cl(1)−Pd(1)−P(2) | 176.20(2) | Cl(2)−Pd(1)−P(1) | 170.53(2) |
| Cl(1)−Pd(1)−Cl(2) | 87.41(2) | Cl(1)−Pd(1)−P(1) | 89.95(2) |
| Cl(2)−Pd(1)−P(2) | 89.82(2) | P(1)−Pd(1)−P(2) | 93.20(2) |
| C(1)−S(1)−C(4) | 91.8(1) | C(5)−S(2)−C(8) | 91.8(1) |
| S(1)−C(1)−C(2) | 112.1(2) | C(1)−C(2)−C(3) | 113.3(2) |
| C(2)−C(3)−C(4) | 111.1(2) | S(1)−C(4)−C(3) | 111.7(2) |

crystals grown from $CH_2Cl_2$/toluene, appears as a toluene adduct (**1-Au-tol**) and does not show any gold−gold interaction (Au−Au distance is 4.685 Å). In solution, only an averaged $^{31}P\{^1H\}$ NMR signal is observed for **1-Au**; there is no significant shift or decoalescence of the singlet in $CD_2Cl_2$ or in $CD_2Cl_2/C_7D_8$ from 183 to 298 K.[31] This result suggests that the gold−gold bond in **1-Au** can be easily

**Scheme 4**

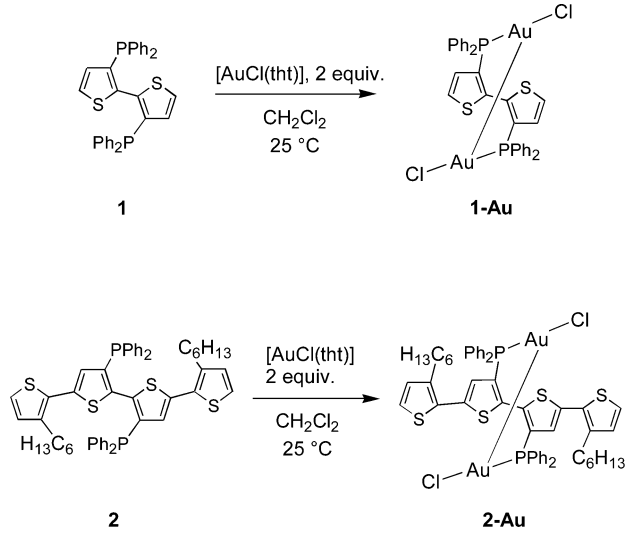


**Table 4.** Selected Bond Lengths and Angles for **2-Pd**

| | | | |
|---|---|---|---|
| | Distances, Å | | |
| Pd(1)−P(1) | 2.2490(9) | S(3)−C(12) | 1.733(4) |
| Pd(1)−P(2) | 2.2510(9) | S(4)−C(16) | 1.699(4) |
| Pd(1)−Cl(1) | 2.3426(9) | S(4)−C(13) | 1.724(4) |
| Pd(1)−Cl(2) | 2.3342(9) | P(1)−C(7) | 1.820(4) |
| S(1)−C(1) | 1.704(4) | P(2)−C(10) | 1.825(3) |
| S(1)−C(4) | 1.732(4) | C(4)−C(5) | 1.470(5) |
| S(2)−C(5) | 1.726(3) | C(8)−C(9) | 1.452(4) |
| S(2)−C(8) | 1.727(3) | C(12)−C(13) | 1.466(5) |
| S(3)−C(9) | 1.721(3) | | |
| | Angles, deg | | |
| P(1)−Pd(1)−P(2) | 93.96(3) | Pd(1)−P(2)−C(10) | 113.77(10) |
| P(1)−Pd(1)−Cl(1) | 86.04(3) | C(9)−S(3)−C(12) | 92.07(16) |
| P(1)−Pd(1)−Cl(2) | 170.38(4) | C(5)−S(2)−C(8) | 92.21(7) |
| Cl(1)−Pd(1)−Cl(2) | 91.30(4) | Pd(1)−P(1)−C(7) | 118.23(10) |
| P(2)−Pd(1)−Cl(1) | 169.06(4) | C(1)−S(1)−C(4) | 91.3(2) |
| P(2)−Pd(1)−Cl(2) | 90.40(3) | C(13)−S(4)−C(16) | 91.98(18) |

(30) Leznoff, D. B.; Xue, B.-Y.; Batchelor, R. J.; Einstein, F. W. B.; Patrick, B. O. *Inorg. Chem.* **2001**, *40*, 6026−6034.

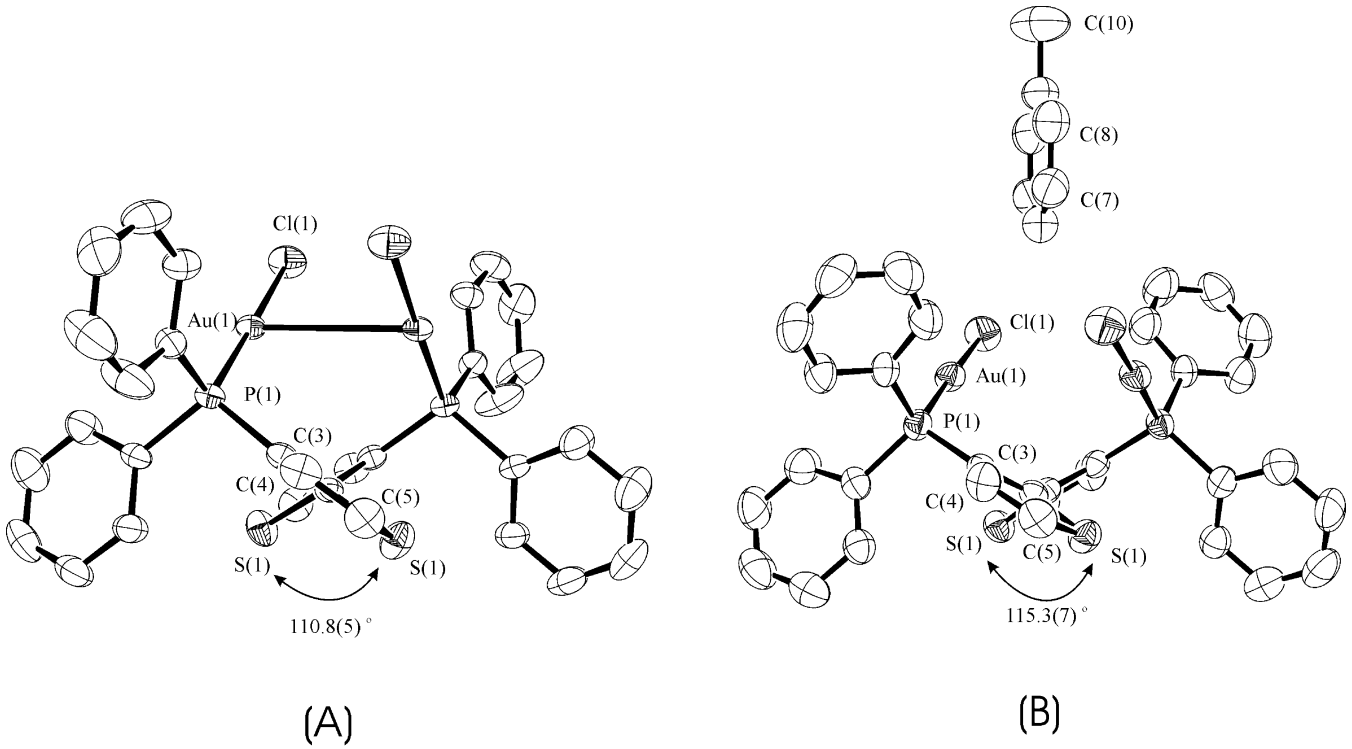


**Figure 4.** (a) ORTEP view of **1-Au**. The hydrogen atoms are omitted for clarity, and thermal ellipsoids are drawn at 50% probability. (b) ORTEP view of **1-Au-tol**. The hydrogen atoms are omitted for clarity, and thermal ellipsoids are drawn at 50% probability.

disrupted by intermolecular forces and is thus quite weak compared to gold−gold interactions in systems such as the auracarborane 1,1′-$(AuPPh_3)_2$-[2-(1′,2′-$C_2B_{10}H_{10}$)-1,2-$C_2B_{10}H_{10}$], for which Au−Au bond strengths of 11 ± 1 kcal/mol have been measured using data obtained from variable temperature $^{31}P\{^1H\}$ NMR.[32]

Selected bond lengths and angles for **1-Au** and **1-Au-tol** are shown in Table 5. For both structures, the average Au−P and Au−Cl bond lengths are comparable with those observed in other phosphinogold(I) halide complexes.[33,34] Given their strong preference for phosphine donors,[34,35] the gold(I) centers do not interact significantly with the thiophene moieties directly, as occurs in related ruthenium(II) complexes.[7,10,36] In the structure of complex **1-Au**, the two planar thiophene rings are oriented S-*anti* to each other with an interannular torsion angle of 110.8(5)°. For **1-Au-tol**, the torsion angle is 115.3(7)°. Thus, despite the lack of a formal Au−Au bond (<3.6 Å), the preferred ligand conformation is similar to **1-Au**. This illustrates that the presence of the gold−gold unit, however weakly interacting, locks the conformation of the thiophene rings into place, as with the palladium(II) systems described. However, in this case, the presence of two metals denies the ligand the ability to form a *cis*-chelate, and instead of being locked into a more planar arrangement as in **1-Pd**, a highly twisted configuration results.

**Table 5.** Selected Bond Lengths and Angles for **1-Au** and **1-Au-tol**

Distances, Å

| | **1-Au** | **1-Au-tol** |
|---|---|---|
| Au(1)−Au(1) | 3.3221(4) | |
| Au(1)−P(1) | 2.230(1) | 2.2244(19) |
| Au(1)−Cl(1) | 2.283(1) | 2.2782(22) |
| P(1)−C(3) | 1.808(5) | 1.800(5) |
| P(1)−C(11) | 1.813(5) | 1.810(6) |
| P(1)−C(21) | 1.815(5) | 1.814(7) |
| C(1)−C(1) | 1.466(9) | 1.465(13) |
| C(2)−C(3) | 1.381(6) | 1.374(8) |
| C(3)−C(4) | 1.419(6) | 1.412(10) |
| C(4)−C(5) | 1.357(8) | 1.343(8) |
| S(1)−C(5) | 1.695(6) | 1.703(8) |
| S(1)−C(2) | 1.722(5) | 1.717(5) |

Angles, deg

| | **1-Au** | **1-Au-tol** |
|---|---|---|
| Cl(1)−Au(1)−P(1) | 178.95(5) | 178.14(6) |
| Au(1)−Au(1)−P(1) | 90.82(3) | |
| Au(1)−Au(1)−Cl(1) | 90.15(4) | |
| Au(1)−P(1)−C(3) | 111.7(1) | 113.23(21) |
| Au(1)−P(1)−C(11) | 114.8(2) | 114.00(24) |
| Au(1)−P(1)−C(21) | 113.6(2) | 113.65(21) |
| P(1)−C(3)−C(4) | 125.9(4) | 123.8(4) |
| P(1)−C(3)−C(2) | 121.1(3) | 124.3(5) |
| C(3)−P(1)−C(11) | 105.6(2) | 105.1(3) |
| C(3)−P(1)−C(21) | 106.5(2) | 104.0(3) |
| C(11)−P(1)−C(21) | 103.9(2) | 105.9(3) |
| C(2)−S(1)−C(5) | 92.5(2) | 92.0(3) |

In a similar fashion, reaction of the quaterthiophene ligand **2** with two equiv of [AuCl(tht)] yielded [(hdppqt)$(AuCl)_2$] (**2-Au**), which showed one singlet in its $^{31}P\{^1H\}$ NMR spectrum at $\delta$ 15.3. The solid-state structure (Figure 5) is

(31) Bardají, M.; Laguna, A. *J. Chem. Educ.* **1999**, *76*, 201−203.
(32) Harwell, D. E.; Mortimer, M. D.; Knobler, C. B.; Anet, F. A. L.; Hawthorne, M. F. *J. Am. Chem. Soc.* **1996**, *118*, 2679−2685.
(33) Leznoff, D. B.; Rancurel, C.; Sutter, J.-P.; Rettig, S. J.; Pink, M.; Paulsen, C.; Kahn, O. *J. Chem. Soc., Dalton Trans.* **1999**, 3593−3599.
(34) Chen, B.-L.; Mok, K.-F.; Ng, S.-C. *J. Chem. Soc., Dalton Trans.* **1998**, 4035−4042.
(35) Fuchita, Y.; Ieda, H.; Wada, S.; Kameda, S.; Mikuriya, M. *J. Chem. Soc., Dalton Trans.* **1999**, 4431−4435.
(36) Weinberger, D. A.; Higgins, T. B.; Mirkin, C. A.; Liable-Sands, L. M.; Rheingold, A. L. *Angew. Chem., Int. Ed.* **1999**, *38*, 2565−2568.

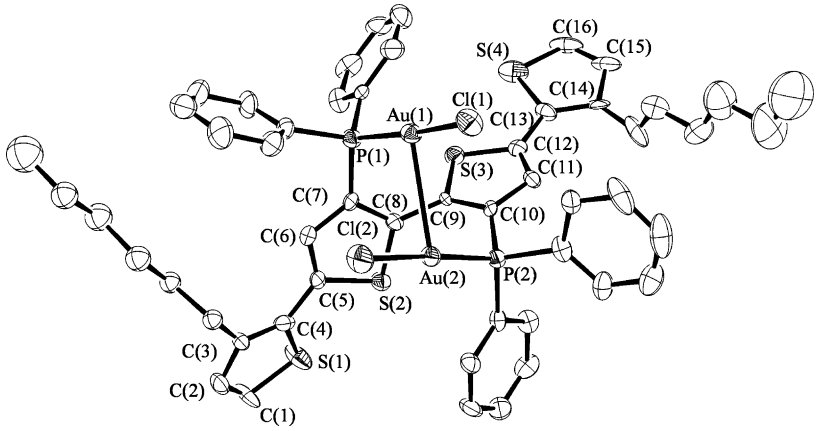


**Figure 5.** ORTEP view of **2-Au**. The hydrogen atoms are omitted for clarity, and thermal ellipsoids are drawn at 50% probability.

**Table 6.** Selected Bond Lengths and Angles for **2-Au**

| Distances, Å | | | |
|---|---|---|---|
| Au(1)−Au(2) | 3.0879(7) | C(9)−C(10) | 1.347(13) |
| Au(1)−P(1) | 2.228(3) | C(10)−C(11) | 1.418(13) |
| Au(2)−P(2) | 2.236(3) | C(11)−C(12) | 1.369(14) |
| Au(1)−C(l1) | 2.286(3) | S(3)−C(9) | 1.711(11) |
| Au(2)−C(l2) | 2.298(3) | S(3)−C(12) | 1.724(11) |
| P(2)−C(10) | 1.833(11) | S(2)−C(5) | 1.730(10) |
| P(1)−C(7) | 1.826(11) | S(2)−C(8) | 1.720(10) |
| C(8)−C(9) | 1.479(13) | C(5)−C(6) | 1.348(13) |
| C(12)−C(13) | 1.468(14) | C(6)−C(7) | 1.414(14) |
| C(5)−C(6) | 1.348(13) | C(7)−C(8) | 1.392(13) |
| C(4)−C(5) | 1.466(14) | | |

| Angles, deg | | | |
|---|---|---|---|
| P(1)−Au(1)−Cl(1) | 174.28(10) | Cl(2)−Au(2)−Au(1) | 85.49(9) |
| P(1)−Au(1)−Au(2) | 95.57(8) | C(9)−S(3)−C(12) | 92.5(5) |
| Cl(1)−Au(1)−Au(2) | 88.16(8) | C(16)−S(4)−C(13) | 91.2(6) |
| P(2)−Au(2)−Cl(2) | 176.87(12) | C(10)−P(2)−Au(2) | 113.3(3) |
| P(2)−Au(2)−Au(1) | 97.63(8) | C(7)−P(1)−Au(1) | 113.5(3) |

similar to **1-Au**, with a quaterthiophene ligand in place of the bithiophene. Bond lengths and angles are collected in Table 6. The Au−Au bond in **2-Au** of 3.0879(7) Å is substantially shorter than that in **1-Au** and likely persists in solution. The deviation from linearity of the Cl−Au−P angle is larger in **2-Au** (174.28°, 176.87°) compared with **1-Au** or **1-Au-tol**, both of which are nearly 179°; this is consistent with the presence of a stronger Au−Au interaction.

Quaterthiophene **2-Au** also has three distinct interannular torsion angles. The central, internal pair of rings are locked with a high twist of 100.8(9)°, similar to the torsional angle in **1-Au** and **3** (110.8(5)° and 124.1(8)°, respectively). The sterically less hindered outer rings are only twisted by 28.5(12)° and 12.5(11)°. Thus, the quaterthiophene unit in **2-Au** can be considered as a pair of bithiophene units. In each unit, the outer thiophene rings are oriented close to a S-*syn* fashion, while the two central rings are oriented S-*anti* to each other. The C(8)−C(9) bond in **2-Au** is longer (1.479(13) Å) than either of the two other interannular C−C bonds in this structure, and longer than these bonds in previously reported quaterthiophenes.[28] This is in contrast to **2-Pd** where the C−C bond between the central two rings is *shorter* than either of the other two interannular bonds. These observations are all consistent with weak conjugation between the two central rings in **2-Au**.

**Spectroscopic and Electrochemical Characterization.** The absorption bands of **1** and **2** are blue-shifted by approximately 50 nm relative to bithiophene (302 nm) and quaterthiophene (390 nm), respectively (Table 7).[37] These shifts may be due to either electronic or steric effects caused by the presence of the phosphines on the oligothiophene units. The negligible shift in absorbance observed for 3′-diphenylphosphino-2,2′:5′2″-terthiophene (dppterth) ($\lambda_{max}$ = 354 nm)[10] relative to terthiophene (355 nm)[37] suggests that the electronic influence of the phosphine group on the oligothienyl moiety is rather small. It is then likely that the larger blue-shifts observed for **1** and **2** are mainly due to twisting between the thiophene rings caused by unfavorable steric interactions between the two phosphine groups. This is supported by the large torsional angle found between the rings in the crystal structure of **3**; it is reasonable that a similar angle would be present in **1** and between the central two rings of **2**.

In complexes **1-Pd** and **2-Pd**, several bands are observed in the UV−vis spectra (Table 7). Related Pd(II) chloro phosphine complexes[38] are known to exhibit C → Pd LMCT bands in the visible region near 340 nm, and such a transition should also be present here, although perhaps shifted slightly in energy; the spectra of both **1-Pd** and **2-Pd** have bands near 340 nm. The presence of the electron-rich oligothiophene ligands indicates that thiophene → Pd LMCT transitions are also expected. The lowest energy bands are tentatively assigned in this way, and the red-shift observed for the lowest energy band in **2-Pd** relative to **1-Pd** supports this assignment. In addition, $\pi-\pi^*$ bands are expected but may be shifted due to a combination of inductive and steric effects resulting from the presence of the metal and phosphine groups. Complete assignment of the bands in the spectra of the Pd complexes is difficult; however, the absorption spectra of the Au complexes are simpler due to the absence of any low energy LMCT bands. In both Au complexes, the spectra are very close to those observed for the respective ligands **1** and **2**. Assuming that the Au does not exert a significant electronic effect, it can be concluded that the torsion angles between the central thiophene rings

(37) Van Pham, C.; Burkhardt, A.; Shabana, R.; Cunningham, D. D.; Mark, H. B.; Zimmer, H. *Phosphorus, Sulfur Silicon Relat. Elem.* **1989**, *46*, 153−168.
(38) Leung, K. H.; Szulbinski, W.; Phillips, D. L. *Mol. Phys.* **2000**, *98*, 1323−1330.

**Table 7.** UV−Vis and Cyclic Voltammetry Data

| complex | UV−vis[a] $\lambda_{max}$/nm ($\epsilon$/$M^{-1}$ $cm^{-1}$) | $E_{p,ox}$[b] V vs SCE | interannular torsion angle ($\theta$)[c] |
|---|---|---|---|
| **1** | 252 (sh) ($3.98 \times 10^4$) | 1.10[d,e] | |
| **2** | 254 ($6.20 \times 10^4$), 340 ($2.83 \times 10^4$) | 1.02[e,f] | |
| **1-Pd** | 258 ($2.51 \times 10^5$), 280 ($2.51 \times 10^5$), 354 (sh) ($4.19 \times 10^4$), 414 (sh) ($9.22 \times 10^3$) | 1.67[d,e] | 51.1(2) |
| **2-Pd** | 267 ($2.06 \times 10^4$), 302 ($1.68 \times 10^4$), 340 (sh) ($1.42 \times 10^4$), 451 ($2.52 \times 10^3$) | 1.40[d,g] | 58.8(3), 56.6(3), 69.0(3) |
| **1-Au** | 239 (sh) ($3.52 \times 10^4$) | >2[d,g] | 110.8(5),[h] 115.3(7)[i] |
| **2-Au** | 252 ($2.88 \times 10^4$), 344 ($1.66 \times 10^4$) | 1.49[d,g] | 28.5(12), 100.8(9), 12.5(11) |
| **3** | 254 ($1.65 \times 10^4$), 286 (sh) ($6.29 \times 10^3$) | >2[e,f] | 124.1(8) |
| 2,2′-bithiophene[j] | 302 ($1.25 \times 10^4$) | 1.31 | 180[k] |
| 2,2′:5′,2″:5″,2‴-quaterthiophene[j] | 390 ($4.55 \times 10^4$) | 0.95 | 181.1(2), 180, 181.1(2)[l] |

[a] In $CH_2Cl_2$. [b] Scan rate = 200 mV/s; only oxidation waves <2 V included. [c] Interannular torsion angle = ∠S−C−C−S. For all quaterthiophene structures, the four linked rings are labeled ABCD, with the torsion angles listed: ∠A−B, ∠B−C, ∠C−D. [d] In $CH_3CN$ containing 0.1 M [(*n*-Bu)$_4$N]$PF_6$. [e] Referenced to decamethylferrocene. [f] In $CH_2Cl_2$ containing 0.1 M [(*n*-Bu)$_4$N]$PF_6$. [g] Referenced to ferrocene. [h] **1-Au**. [i] **1-Au-tol**. [j] UV−vis, ref 37; cyclic voltammetry, ref 40. [k] Ref 42. [l] Ref 43.

are similar in the Au complexes to those in the respective ligands. Indeed, the torsion angles in **1-Au** and the phosphine oxide **3** are reasonably comparable.

Both **1** and **2** have a first oxidation potential close to that observed for the oxidation of $PPh_3$, which has been assigned to formation of the triphenylphosphonium cation followed by reaction with trace water to give triphenylphosphine oxide.[39] In phosphine oxide **3**, the oxidation wave is shifted to a much more positive potential than in bithiophene, due to the electron-withdrawing effect of the phosphine oxide group on the conjugated system, and to the large deviation from planarity in **3**.

The cyclic voltammogram of **1-Pd** contains an irreversible oxidation wave (Table 7) assigned to an oligothiophene-based process; no analogous wave is observed for **1-Au** below 2 V. For both complexes, oxidation occurs significantly positive of bithiophene (+1.31 V).[40] There are two factors which can contribute to this shift: (a) the inductive effect of the metal and (b) the change in the interannular conjugation which results upon coordination. In **1-Pd**, both the electron-withdrawing effect of the $PdCl_2$ group[41] and the large torsion angle relative to bithiophene result in the observed increase in the oxidation potential relative to bithiophene. In **1-Au**, the interannular torsion angle is substantially larger than in **1-Pd**, and comparable to that in **3**. In solution, rotation between rings may be allowed; however, the fully planar *anti* conformation is also unlikely in this case due to unfavorable steric interactions. In this case, it is likely that the shift to higher oxidation potential relative to **1-Pd** results from poorer conjugation between thiophene rings as seen in the larger torsion angle. This is supported by the longer intrannular C−C bonds (vide supra) in **1-Au** versus **1-Pd**.

The CVs of compounds **2-Pd** and **2-Au** also contain irreversible oxidation waves, assigned to ligand-based processes (Table 7). Generally, extending the length of a $\pi$-system results in a decrease in the oxidation potential.[40] This effect is observed in both sets of complexes where extension from two to four rings results in a decrease in oxidation potential. The crystal structure of **2-Au** shows that the outer two thiophene rings are close to coplanar; thus, the presence of the metal groups results in these complexes behaving like two bithiophene units that are weakly conjugated to each other.

When the working electrode was scanned repeatedly past the first oxidation wave in solutions of the complexes **1-Pd**, **1-Au**, **2-Pd**, or **2-Au**, there was no evidence of film formation on the electrode surface. There are two possible reasons why these complexes did not electropolymerize. First, the interannular twisting which results in blue-shifted absorption peaks and higher oligothiophene oxidation potentials may be severe enough to prevent any coupled materials that form from being sufficiently conductive to allow film growth. Second, the solid-state structures of **1-Pd** and **1-Au** indicate that the phenyl rings of the phosphines extend past the α-positions of the bithienyl moieties, which may reduce their accessibility for coupling. The quaterthiophene complexes should not be influenced by this effect, so in **2-Au** and **2-Pd**, it is likely that the interannular twisting observed in the crystal structures is sufficient to prevent conductivity along the backbone and growth of a conductive film.

## Conclusions

Binding bulky metal groups to oligothiophenes via chelating phosphines results in substantial effects on the electronic properties of the conjugated system. Perturbations result from a combination of factors including changes in the interannular torsion angles due to the backbone substituents and the metal groups, as well as inductive effects. The interannular torsion angles in the complexes examined here are large relative to those typically observed in solid-state structures of oligothiophenes.[28] In the metal complexes, both blue-shifts in the $\pi-\pi^*$ absorption bands and increases in the oxidation

(39) Schiavon, G.; Zecchin, S.; Cogoni, G.; Bontempelli, G. *J. Electroanal. Chem. Interfacial Electrochem.* **1973**, *48*, 425−431.
(40) Diaz, A. F.; Crowley, J.; Bargon, J.; Gardini, G. P.; Torrance, J. B. *J. Electroanal. Chem.* **1981**, *121*, 355−361.
(41) Corain, B.; Longato, B.; Favero, G.; Ajò, D.; Pilloni, G.; Russo, U.; Kreissl, F. R. *Inorg. Chim. Acta* **1989**, *157*, 259−266.
(42) Pelletier, M.; Brisse, F. *Acta Crystallogr., Sect. C* **1994**, *50*, 1942−1945.
(43) Antolini, L.; Horowitz, G.; Kouki, F.; Garnier, F. *Adv. Mater.* **1998**, *10*, 382−385.

potentials of the oligothiophene $\pi$-system due to the large interannular torsion angles are observed, relative to unsubstituted oligomers. As expected, increasing the length of the conjugated system from two to four rings resulted in a decrease in oxidation potential, and a red-shift in the absorption spectrum for both the Pd and the Au complexes.

These results suggest that the electronic behavior of polythiophenes incorporating similar pendant metal groups into the backbone would be drastically influenced by the presence of these moieties. We are currently investigating alternatives to electropolymerization to prepare these extended materials.

**Acknowledgment.** M.O.W. and D.B.L. thank the Natural Sciences and Engineering Research Council of Canada and D.B.L. thanks Simon Fraser University and Meiji University for support of this research.

**Supporting Information Available:** X-ray crystallographic data files (CIF) for **3**, **1-Pd**, **2-Pd**, **1-Au**, **1-Au-tol**, and **2-Au**. Fully labeled ORTEP views of all crystal structures (PDF). This material is available free of charge via the Internet at http://pubs.acs.org.

IC0258328